BASIC RESEARCH PAPER

Autophagy 6:2, 1-15; February 16, 2010; © 2010 Landes Bioscience

Carcinoma cells activate AMP-activated protein kinase-dependent autophagy as survival response to kaempferol-mediated energetic impairment

Giuseppe Filomeni,[1,†] Enrico Desideri,[1,2,†] Simone Cardaci,[1] Ilaria Graziani,[1] Sara Piccirillo,[2] Giuseppe Rotilio[1,2] and Maria R. Ciriolo[1,2,*]

[1]Department of Biology; University of Rome "Tor Vergata"; Rome, Italy; [2]Research Centre IRCCS San Raffaele Pisana; Rome, Italy

[†]These authors contributed equally to this work.

Key words: kaempferol, mitochondria, glucose uptake, bio-energetics, autophagy, apoptosis, AMPK, mTOR

Abbreviations: AMPK, AMP-activated protein kinase; Atg5, autophagy-related 5 homolog; 2-DG, 2-deoxy-D-glucose; 2-NBDG, 2-[N-(7-nitrobenz-2-oxa-1,3-diazol-4-yl)amino]-2-deoxy-D-glucose; 3-MA, 3-methyladenine; DHDCF-DA, 2',7'-dihydrodichlorofluorescein diacetate; DMSO, dimethyl sulfoxide; EGFP, enhanced green fluorescent protein; GAPDH, glyceraldehyde-3-phosphate dehydrogenase; LC3, microtubule-associated protein light chain 3; MAPK, mitogen activated protein kinase; mTOR, mammalian target of rapamycin; NAC, N-acetylcysteine; OXPHOS, oxidative phosphorylation; PARP, poly-ADP ribose polymerase; ROS, reactive oxygen species; siRNA, small interference RNA; zVAD-*fmk*, benzyloxycarbonyl-Val-Ala-Asp-fluoromethyl ketone

Kaempferol, a dietary cancer chemopreventive polyphenol, has been reported to trigger apoptosis in several tumor histotypes, but the mechanism underlying this phenomenon is not fully understood. Here, we demonstrate that in HeLa cells, kaempferol induces energetic failure due to inhibition of both glucose uptake and Complex I of the mitochondrial respiratory chain. As adaptive response, cells activate autophagy, the occurrence of which was established cytofluorometrically, upon acridine orange staining, and immunochemically, by following the increase of the autolysosome-associated form of the microtubule-associated protein light chain 3 (LC3-II). Autophagy is an early and reversible process occurring as survival mechanisms against apoptosis. Indeed, chemical inhibition of autophagy, by incubations with monensin, wortmannin, 3-methyladenine, or by silencing Atg5, significantly increases the extent of apoptosis, which takes place via the mitochondrial pathway, and shortens the time in which the apoptotic markers are detectable. We also demonstrate that autophagy depends on the early activation of the AMP-activated protein kinase (AMPK)/mTOR-mediated pathway. The overexpression of dominant negative AMPK results in a decrease of autophagic cells, a decrement of LC3-II levels, and a significant increase of apoptosis. Experiments performed with another carcinoma cell line yielded the same results, suggesting for kaempferol a unique mechanism of action.

Introduction

Cancer cells need a higher amount of energy to allow survival in restrictive conditions (e.g., low pH and oxygen concentrations).[1] However, they show a predominant glycolytic flux if compared with differentiated cells which, conversely, rely upon oxidative phosphorylation (OXPHOS) for most of their energy.[1] The metabolic switch from OXPHOS to glycolysis is better known as aerobic glycolysis or "Warburg effect."[2] However, also under aerobiosis, glycolysis-derived ATP in tumors is between 2% and 60% of the total ATP produced.[3,4] Therefore, to improve therapeutic activity and selectivity of anticancer drugs, many glycolytic inhibitors have been developed and their anticancer property has been investigated. Among them, there are: (i) gossypol, a drug that blocks glycolysis by inhibiting NAD^+-dependent enzymes,[5] and (ii) 2-deoxy-D-glucose (2-DG), a glucose analogue phosphorylated by hexokinase, but not further metabolized by phosphoglucose isomerase.[6] Although an increased glycolytic rate is required for proliferation,[7] this strategy has only moderate effects in those cancer cells, like HeLa cells, which generate ATP mainly through OXPHOS.[8] In this case, a more successful strategy is based on the simultaneous blockage of glycolysis and OXPHOS pathways by a combined use of inhibitors, e.g., Rhodamine 123, an OXPHOS uncoupler, together with 2-DG;[9] or by using a specific inhibitor

*Correspondence to: Maria Rosa Ciriolo; Email: ciriolo@bio.uniroma2.it
Submitted: 09/29/09; Revised: 12/10/09; Accepted: 12/17/09
Previously published online: www.landesbioscience.com/journals/autophagy/article/10971

of both glycolysis and OXPHOS, such as 3-bromopyruvate.[10,11] However, it is well known that during tumor invasion, cancer cells show high tolerance to nutrient deprivation because of their excessive demand for nutrition and oxygen without neovascularization. In particular, it has been demonstrated that nutrient starvation in vitro is a key factor for tumor progression,[12] and that AMP-activated protein kinase (AMPK) plays a major role in protecting tumor cells from metabolic stresses.[13]

AMPK is an evolutionary conserved heterotrimeric kinase regulated by alterations in cellular energetic status. Increase of AMP/ATP ratio leads to conformational changes of AMPK that renders the protein accessible for the phosphorylation on Thr^{172} by the upstream kinases, such as LKB1 and Calcium/calmodulin-dependent protein kinase kinase (CaMKK).[14] Once phosphorylated, AMPK is active and stimulates the pathways converging in the generation of ATP by phosphorylation of specific substrates (enzymes and transcription factors). Among the substrates phosphorylated by AMPK, there are several enzymes involved in glycolysis, fatty acid metabolism and mitochondrial biogenesis.[14] Moreover, a role for AMPK in the activation of the mitogen activated protein kinases (MAPK), or in the inhibition of mammalian target of rapamycin (mTOR) pathway has also emerged.[15] Therefore, a more general implication of AMPK in regulating cell fate by influencing autophagy and apoptosis should be considered.

Flavonoids are a huge class of polyphenols largely distributed in plants. Flavonoids mostly derive from benzo-γ-pyrone and can be divided into 14 sub-classes that differ for substituting groups of ring A, B and C.[16] Among the members of the sub-class of flavonols, the most common compounds are quercetin, myricetin and kaempferol. Many studies demonstrated that flavonoids have high antioxidant properties,[17,18] which explain why their consumption is often associated with a reduced risk of cancer and cardiovascular diseases.[19,20] Moreover, at pharmacological concentrations, flavonoids are also able to act as pro-oxidants and to induce apoptosis, thus behaving as promising therapeutic agents to be used as co-adjuvant in cancer treatment.[21-23] The general mechanism of action of polyphenols involves the activation of pro-apoptotic members of MAPK, but a comprehensive analysis of their cellular effects has not been reported yet. In this study, we describe the capability of kaempferol to affect glucose uptake prior to inhibition of the mitochondrial electron transfer chain, and how the resulting energetic stress is buffered by the activation of autophagy via the AMPK/mTOR-mediated pathway.

Results

Kaempferol affects glucose uptake and inhibits mitochondrial respiration. Kaempferol is a flavonol recently proposed to exert antiproliferative effects on tumors.[24] Since the inhibition of glucose uptake has been proposed to occur upon treatment with various polyphenols,[25,26] we wondered whether this event was also involved in kaempferol treatment. We treated HeLa cells with 100 and 200 μM kaempferol, concentrations similar to those employed in other studies regarding the toxic effects of kaempferol,[27,28] and measured lactate levels in culture media. Histograms depicted in **Figure 1A** show that in the first 6 h of treatment extracellular lactate was significantly reduced, a phenomenon that was dependent on the concentration of either kaempferol or glucose in culture media. Indeed, cells cultured in low-glucose (5.6 mM) were much more affected by kaempferol treatment than those cultured in normal, high-glucose (25 mM), D-MEM. Therefore, to evaluate directly the efficiency of glucose uptake, we performed experiments in the presence of 100 μM 2-NBDG, a fluorescent non-metabolizable analogue of glucose. **Figure 1A** shows that HeLa cells treated with 200 μM kaempferol for 30 min were less fluorescent than untreated cells. Moreover, cytofluorometric evaluations pointed out that kaempferol-treated cells showed a 61 ± 4% decrease of 2-NBDG uptake with respect to untreated cells (**Fig. 1A**).

Changes in the glycolytic pathway could affect the mitochondrial OXPHOS; therefore, we performed analyses of oxygen consumption on HeLa cell suspension. Six hour-treatment with 200 μM kaempferol did not produce significant changes in respiration rate (data not shown). Conversely, 12 h-treatment showed a significant decrease of total oxygen consumption (4.51 ± 0.43 vs. 7.35 ± 0.25 nmol O atom x min^{-1} x mg $prot^{-1}$, n = 5, $p < 0.01$). To determine which complex of the mitochondrial transfer chain was mainly affected, we analyzed oxygen consumption by each Complex upon permeabilization of the cells with digitonin after 12 h of treatment. **Figure 1B** shows that kaempferol specifically affected NADH-dependent mitochondrial respiration at Complex I, whereas no significant inhibition was obtained for the other mitochondrial components. We then moved on to purified mitochondria from mouse liver and used them to assess whether kaempferol could directly influence electron transfer chain. Oxygen consumption was determined upon the addition of 50 μM kaempferol in the buffer assay containing purified mitochondria. Succinate-dependent respiration was not significantly affected by kaempferol (data not shown), whereas oxygen consumption was inhibited when NADH was added in experimental buffer containing glutamate/malate. **Figure 1C** shows that total oxygen consumption significantly decreased (6.72 ± 1.83 versus 12.10 ± 3.12 nmol O atom x min^{-1} x mg $prot^{-1}$, n = 5, $p < 0.01$), indicating that kaempferol is able to hinder mitochondrial respiration at the level of Complex I.

On the basis of these results, we wondered whether total ATP content could be affected by kaempferol; therefore cells were treated with 200 μM kaempferol up to 24 h, and ATP evaluated. A significant reduction of ATP content was determined after 12 h-treatment in low-glucose conditions, while no significant change were observed when the cells were grown in normal medium (high-glucose) (**Fig. 1D**).

Metabolic stress induced by kaempferol activates autophagy. The energetic failures induced by kaempferol can be associated with the activation of autophagy as a survival mechanism. This protective response results in resistance to the toxic effects of drugs that elicits cell death by creating metabolic stress.[29] We then investigated the possibility that HeLa cells underwent autophagy as adaptive response to kaempferol-mediated energetic stress. **Figure 2A** shows optic microscopy images of a typical morphology of HeLa cells after 12 h-treatment with 200 μM

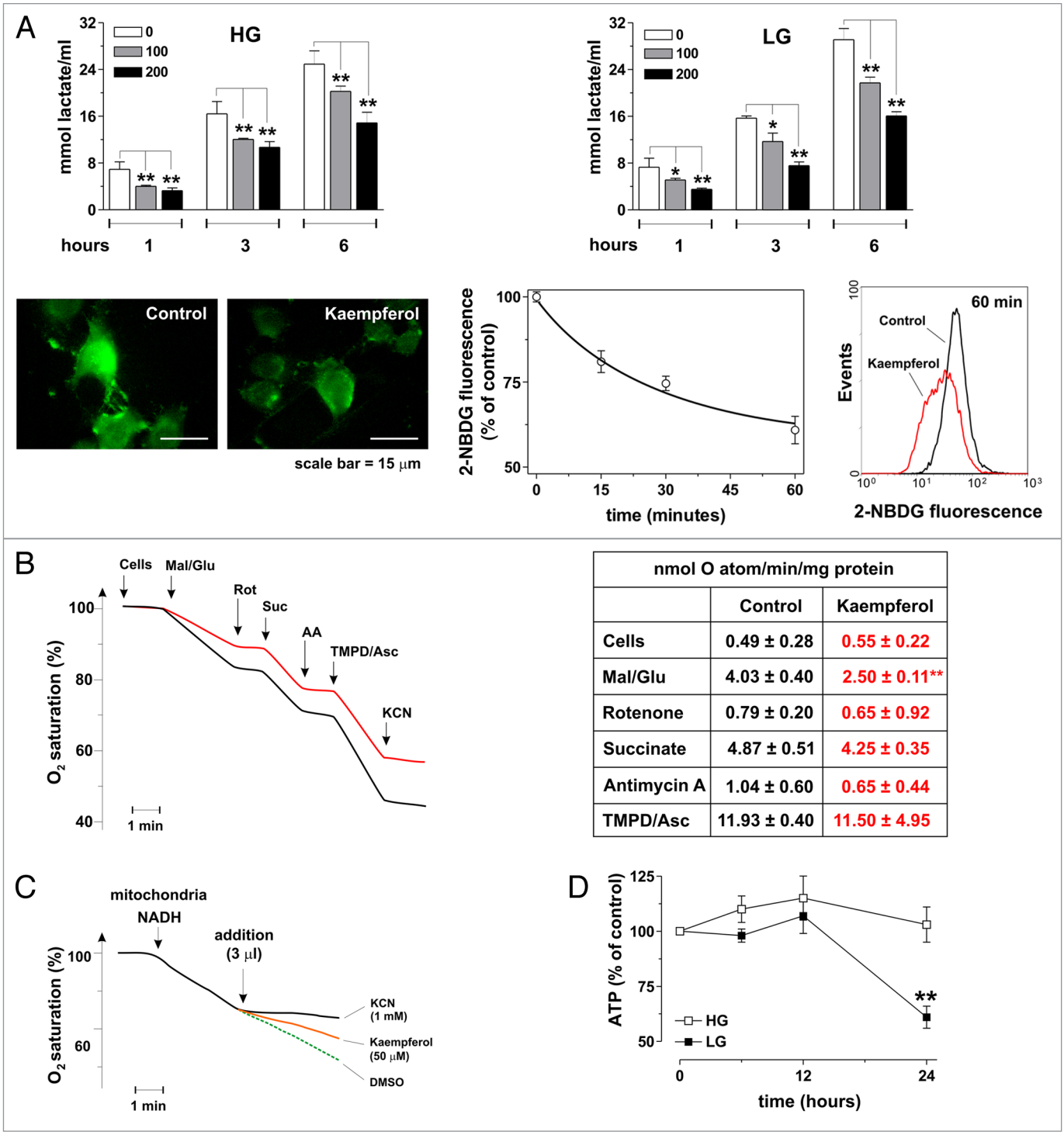

nmol O atom/min/mg protein		
	Control	Kaempferol
Cells	0.49 ± 0.28	0.55 ± 0.22
Mal/Glu	4.03 ± 0.40	2.50 ± 0.11**
Rotenone	0.79 ± 0.20	0.65 ± 0.92
Succinate	4.87 ± 0.51	4.25 ± 0.35
Antimycin A	1.04 ± 0.60	0.65 ± 0.44
TMPD/Asc	11.93 ± 0.40	11.50 ± 4.95

Figure 1. For figure legend, see page 4.

kaempferol. The same phenotype was evidenced even at low concentrations, with the number of shrinking cells decreasing in a dose-dependent manner (data not shown). HeLa cells were then transfected with a vector expressing the EGFP-conjugated microtubule-associated protein 1 light chain 3 (LC3), treated for 12 h with kaempferol and monitored for the presence of dotted fluorescence. **Figure 2B** shows discrete green spots, which reasonably represent autolysosomes,[30] with the cells grown in low-glucose being more autophagic than those cultured under high-glucose. Colocalization analyses of LC3 and lysosomes stained with the lysosome-specific probe LysoTracker Red® shows that LC3 co-localized with lysosomes, especially at 12 h of treatment (**Fig. 2C**). We then attempted to measure cytofluorometrically the extent of autophagic cells taking advantage of acridine orange staining.[11,31]

Figure 1. Effects of kaempferol on cellular energetics. (A) HeLa cells grown in medium containing 25 mM (*HG*), or 5.6 mM glucose (*LG*) were treated with 100 or 200 μM kaempferol up to 6 h. At indicated times, cell media were collected and lactate determined spectrophotometrically following the reduction of NAD^+ at 340 nm. Data are expressed as nmoles of lactate/ml and represent the mean ± SD of n = 12 independent experiments. *p < 0.05; **p < 0.01. Moreover, HeLa were incubated with 100 μM 2-NBDG and treated with 200 μM kaempferol. After 30 min cells were washed to stop 2-NBDG uptake, collected and fluorescence analyzed by fluorescence microscopy (left). Similarly, cells were analyzed cytofluorometrically after 15, 30 and 60 min and the percentage of decrease with respect to untreated cells analyzed by a WinMdi 2.8 software. A representative cytofluorometric histogram obtained after 60 min of treatment is shown (right). (B) HeLa cells were treated for 12 h with 200 μM kaempferol, rinsed, detached and counted to reach a concentration of 1 x 10^7 cells/ml in "measurement" buffer. Oxygen consumption of untreated (black draw) or kaempferol-treated cells (red draw) was then measured upon incubation with digitonin. 5 mM malate and glutamate (*Mal/Glu*), 5 mM succinate (*Suc*), 0.5 mM TMPD and 2 mM ascrbate (*TMPD/Asc*) were added as substrates of Complex I, II and IV, respectively. 100 nM rotenone (*Rot*), 1 μM antimycin A (*AA*) and 1 mM KCN were added to selectively inhibit Complex I, III and IV, respectively. Table on the right shows the values of oxygen consumption expressed as nmol of atomic oxygen/min/mg protein and represents the mean ± SD of n = 4 independent experiments. **p < 0.01. (C) 1 mg/ml of mouse liver mitochondria was incubated in experimental buffer supplemented of 1 mM NADH. Where indicated, 50 μM kaempferol (red draw), or 1 mM KCN (black draw) were added to mitochondrial suspension. DMSO (dotted green draw) was used as negative control. (D) HeLa cells, cultured in HG or LG media were treated with 200 μM kaempferol. At indicated times, cells were harvested and used for ATP measurement. Data are expressed as percentage of control and represent the mean ± SD of n = 12 independent experiments. **p < 0.01.

Figure 2D shows that the percentage of cells emitting in bright red fluorescence (autophagic) increased in a time-dependent manner, and to a different extent depending on growth conditions. We also performed western blot analyses of LC3 in HeLa cells treated with increasing doses of kaempferol. **Figure 2E** shows that resting HeLa cells shows a marked expression of the immune-reactive band representative of LC3-II if compared with other cells lines (e.g., neuroblastoma cells SH-SY5Y), however treatments with kaempferol induced a dose and time-dependent increase of LC3 II, with HeLa cells grown in low-glucose being the most responsive.

HeLa cells activate autophagy as survival response to kaempferol. The role of autophagy was investigated by incubating HeLa cells with wortmannin and 3-MA that inhibit class III phosphatidylinositole-3-phosphate kinases, which are responsible for the early phases of autophagy,[32,33] or with monensin, an ionophore impeding the late fusion between lysosomes and phagosomes.[34] Under these conditions, 24 h-treatment with 200 μM kaempferol resulted in a massive cell detachment from the flasks, which seemed to be much more evident in cells grown in low-glucose. Therefore, we stained the cells with propidium iodide and analyzed the occurrence of apoptosis by cytofluorometric analyses in both cell growth conditions. As expected, chemical inhibition of autophagy with wortmannin, 3MA or monensin completely abolished acridine orange positive cells (**Suppl. Fig. 1**) and concomitantly resulted in a massive induction of apoptosis (**Fig. 3A–C**), the extent of which was also related to the presence of glucose in culture media. We then transfected the cells with an siRNA against autophagy-related gene 5 homolog (siAtg5 cells), a protein involved in the early stages of autophagosome formation,[35] or with a scramble siRNA duplex (siScr). **Figure 3D** shows that, under these conditions, siAtg5 cells were committed to apoptosis with an extent of about 40%. These results confirmed that the activation of autophagy in response to kaempferol is a survival response.

In order to generalize the processes underlying kaempferol toxicity against carcinoma cell growth, we selected another carcinoma cell line, the gastric adenocarcinoma AGS. Results obtained with AGS mirrored those achieved in HeLa cells. In particular, a typical shrinkage of the cytoplasm and a significant increase of autophagic cells were evidenced upon treatment with kaempferol. This phenomenon, which was reverted by siRNA against Atg5, was also associated with a considerable increase of LC3-II immuno-reactive band and with its redistribution in discrete spots (likely auto-phagolysosomes) (**Suppl. Fig. 2A–E**).

To verify that autophagy played a protective role under our experimental conditions, we performed pulse-chase experiments consisting in treating HeLa cells with 200 μM kaempferol for different times, after which the medium was replaced and the cells cultured up to 48 h in fresh medium. **Figure 4A** shows that kaempferol removal after 12 h-treatment rescued cells from apoptosis. Conversely, when the replacement of the medium was carried out after 24 h, an increase of apoptotic cells at 48 h to values close to 40% was reached. These results confirmed that 24 h was the time where cell survival seems to be completely compromised and autophagy no more able to repress the apoptotic machinery. Next, HeLa cells treated for 6 and 12 h with kaempferol, were rinsed with fresh medium, reseeded in kaempferol-free milieu and cell growth monitored for further 48 h by direct counts upon Trypan blue exclusion. **Figure 4B** shows that the amount of apoptotic cells did not increase after reseeding. Moreover, viable cells after kaempferol removal still remain viable and were able to replicate, confirming that autophagy was a protective event upon kaempferol-mediated insult (**Fig. 4C**).

Prolonged incubations with kaempferol result in ROS-dependent and MAPK-mediated apoptosis. We analyzed whether chronic incubation with kaempferol resulted in apoptosis by cytofluorometric analyses of HeLa cells, upon staining with propidium iodide. Histograms depicted in **Figure 5A** show cell cycle distribution of cells treated for 48 h with different concentrations of kaempferol. Under these conditions, a dose-dependent (between 50 and 200 μM) increase in the percentage of $subG_1$ (apoptotic) cells was evidenced. We characterized the apoptotic pathway by evaluating the levels of pro- and active caspase-9, caspase-8, as well as caspase-3 and poly-ADP ribose polymerase (PARP) by western blot analyses. Results reported in **Figure 5B** show that each step of the intrinsic apoptotic program (caspase 9-mediated) was executed, whereas no activation of the receptor-dependent apoptosis (caspase 8-mediated) seemed to occur under our experimental conditions. Conversely, western blots performed after 24 h-treatment indicated that this was the time sufficient to induce only the cleavage of caspase-9, but not the proteolysis of

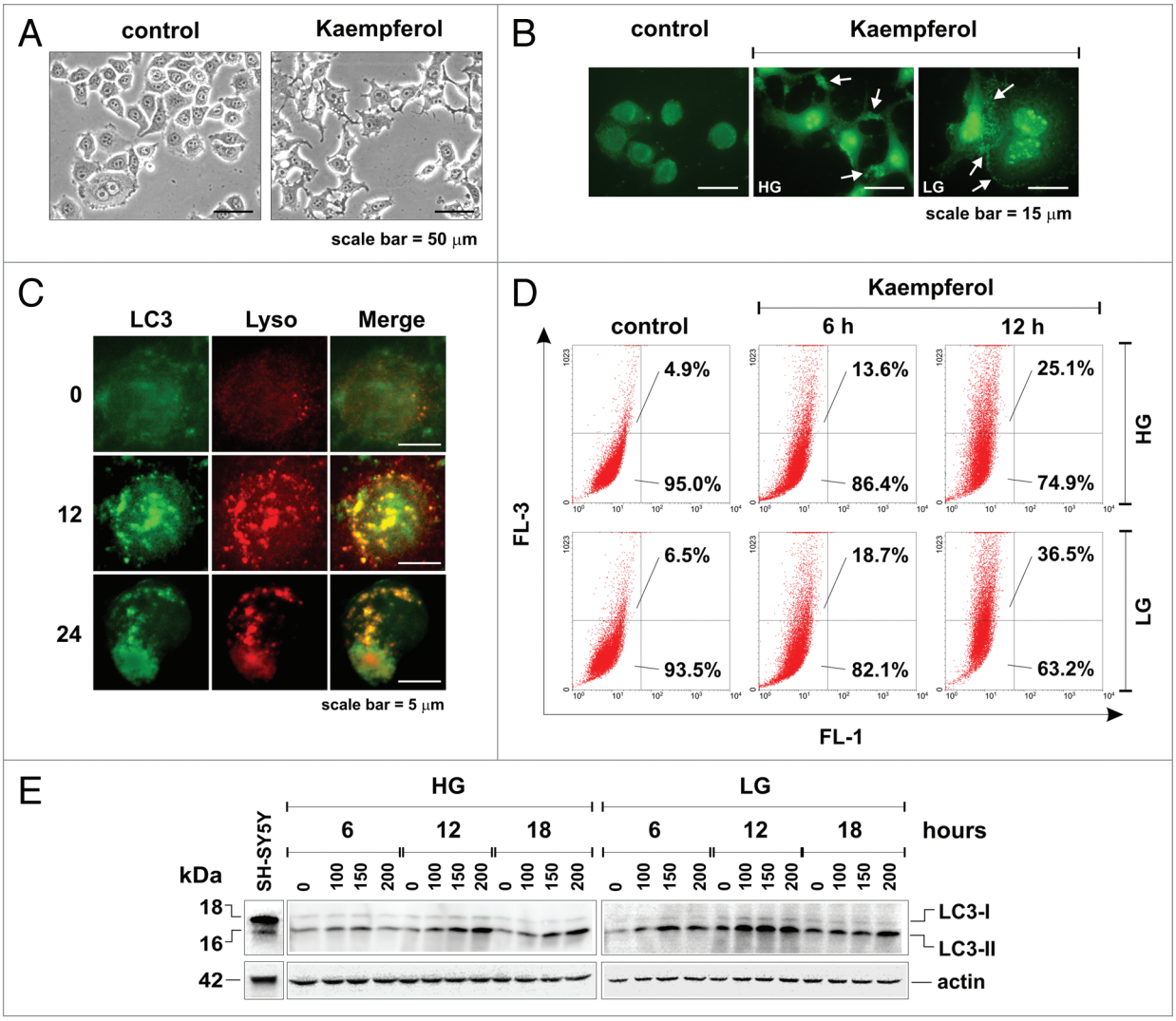

Figure 2. Effects of kaempferol on autophagy commitment. (A) HeLa cells were treated with 200 μM kaempferol for 12 h and the morphology visualized directly on viable cells by optic microscopy. (B) Alternatively, they were transfected with EGFP-LC3-containing plasmid. After two days in HG or LG media, they were seeded onto coverslips, treated with 200 μM kaempferol for 12 h and fixed with 4% paraformaldehyde. Images were digitized with a Cool Snap video camera connected to Nikon Eclipse TE200 fluorescence microscopy (*white arrows*, green spots). (C) For autophagy determination, EGFP-LC3 transfected cells were incubated for 30 min with 75 nM Lysotracker Red® before fixation and images digitized with a Delta Vision Restoration Microscopy System equipped with an Olympus IX70 fluorescence microscope. (D) Alternatively, HeLa cells were treated with 200 μM kaempferol for 6 and 12 h, incubated with 500 nM acridine orange for 15 min, washed, detached and collected in PBS. Data are expressed as percentage of autophagic (upper left) and nonautophagic (lower left) cells and are representative of n = 4 independent experiments that gave similar results. (E) HeLa cells cultured in HG or LG media were treated with different concentrations of kaempferol. At indicated times, 75 μg of total protein extract was loaded onto each lane for detection of basal (LC3-I) and phosphatidyl-ethanolamine-conjugated form of LC3 (LC3-II). Actin was used as loading control. Western blots are from one experiment representative of three that gave similar results. On the left immunoreactive bands of LC3-I and LC3-II from neuroblastoma cell line SH-SY5Y are reported.

PARP, which became evident at 36 h (**Fig. 5C**). We then inhibited caspase activity by means of incubations with 20 μM of the pan-caspase inhibitor zVAD-*fmk*. **Figure 5D** shows that when caspase activity was inhibited (**Suppl. Fig. 3**), the extent of apoptotic cells proportionally decreased, indicating that apoptosis was a caspase-dependent event. In the attempt to identify the switch between autophagy and apoptosis, we focused on the possible involvement of oxidative stress and the death pathways dependent on it. HeLa cells were treated with 200 μM kaempferol and analyzed cytofluorometrically for ROS production. **Figure 6A** shows that no significant change in ROS levels was evaluated during 12 h-treatment, whereas a sustained increase became evident between 18 and 24 h, time points consistent with the appearance of the early apoptotic markers. We then assessed whether ROS increase could be the event responsible for the activation of the pro-apoptotic members of MAPK family, JNK and $p38^{MAPK}$, that are known to be responsive to redox changes and reported to be activated by other polyphenols.[36] **Figure 6B** shows that phospho-active levels of $p38^{MAPK}$ did not increase during treatment with kaempferol, whereas phospho-JNK immunoreactive

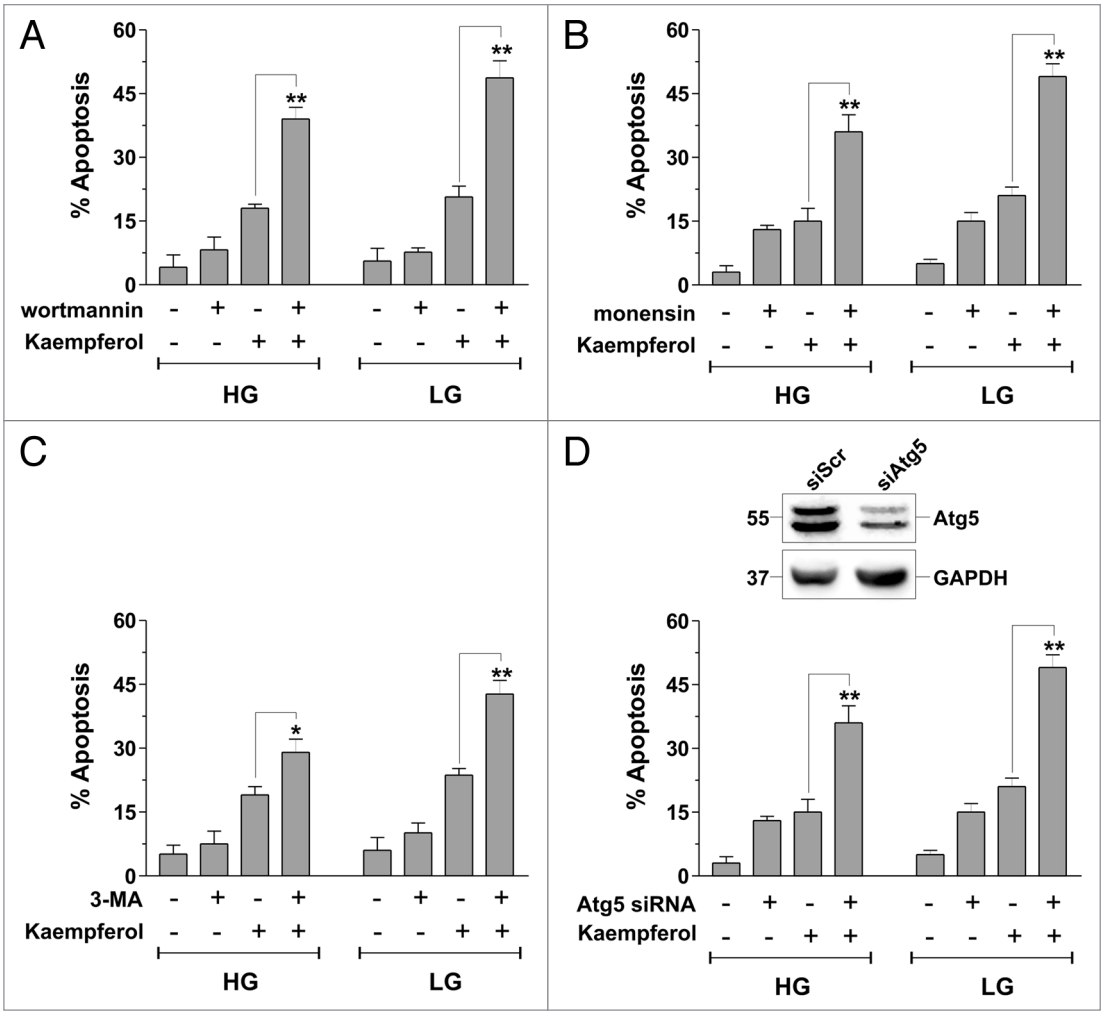

Figure 3. Effects of autophagy inhibitors. (A) HeLa cells cultured in HG or LG media were incubated for 1 h with 1 μM wortmannin, or (B) with 2.5 μM monensin, or (C) with 10 mM 3-MA to inhibit autophagy, treated with 200 μM kaempferol for 24 h and stained with propidium iodide. (D) Cells were transiently transfected with siRNA Atg5 mRNA target sequence (*siAtg5*) or with a scramble siRNA duplex (*siScr*). After 24 h from transfection, siScr and siAtg5 cells were harvested and lysed. Twenty-five μg of total protein extract was loaded onto each lane for detection of Atg5. GAPDH was used as loading control. Western blots are from one experiment representative of three that gave similar results. Concomitantly, after 24 h from transfection, siScr and siAtg5 cells cultured in HG or LG media were treated with 200 μM kaempferol for further 24 h, harvested and analyzed cytofluorometrically for apoptotic extent. Data are expressed as percentage of apoptotic cells and represent the mean ± SD of n = 6 independent experiments. **p < 0.01.

bands became significantly higher than control at 18 and 24 h, time points correlating with the appearance of ROS. On the basis of these results, we treated the cells with kaempferol, and only after 12 h we added the well-known thiol antioxidant NAC (5 mM), or the chemical inhibitor of JNK, SP600125 (10 μM), and evaluated the extent of apoptosis after 24 h. **Figure 6C** shows that both compounds significantly protected HeLa cells against kaempferol-mediated apoptosis, confirming the role of the redox activation of JNK in such an event.

Inhibition of glucose uptake and complex I is required for the induction of autophagy and sensitization to kaempferol. To connect kaempferol-mediated metabolic stress and autophagic response, we cultured HeLa cells in low-glucose medium and analyzed cell viability at longer time points (36 and 48 h). **Figure 7A** shows that cells were more susceptible to kaempferol-mediated apoptosis, a result also confirmed by western blot analyses of PARP (**Suppl. Fig. 4**). Next we pre-incubated the cells for 1 h with 10 mM sodium pyruvate to overcome glucose deprivation-dependent impairment of glycolysis; then kaempferol was added and apoptosis measured cytofluorometrically. **Figure 7B** shows that pyruvate partially protected the cells from apoptosis after 36 h of treatment with 200 μM kaempferol. Nevertheless, such protection was lost at 48 h, confirming that refueling mitochondria with pyruvate is not sufficient to overcome kaempferol-mediated mitochondrial failure. Since Complex I was the main mitochondrial target of kaempferol, we further incubated the cells with 20 mM methyl succinate, a cell permeable substrate of Complex II and, then, added kaempferol. **Figure 7C** shows a significant protection of methyl succinate towards kaempferol-induced toxicity either at 36 or 48 h-treatment suggesting that fuel supplying to succinate dehydrogenase could revert cell demise. These results pointed out the existence of at least two distinct processes

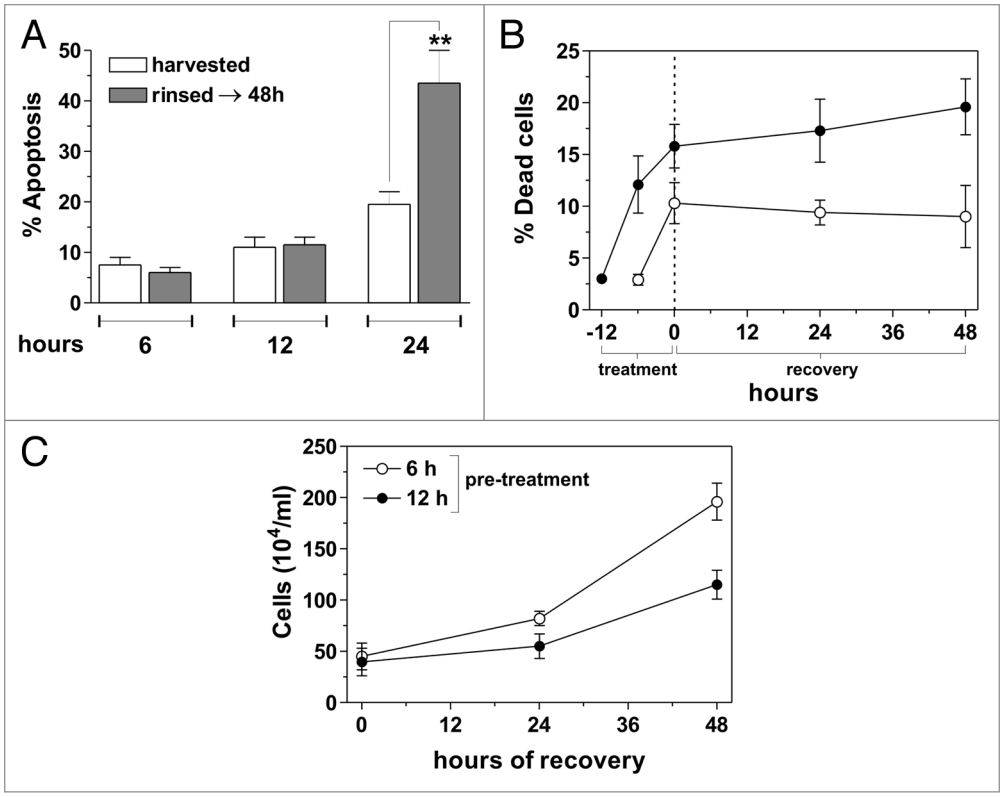

Figure 4. Survival role of autophagy. (A) HeLa cells were treated with 200 μM kaempferol for 6, 12 or 24 h. At indicated times cells were harvested and analyzed cytofluorometrically for apoptotic extent (white histograms), or alternatively washed and maintained in culture up to 48 h (grey histograms). Data are expressed as percentage of apoptotic cells and represent the mean ± SD of n = 4 independent experiments. **p < 0.01. Alternatively, HeLa cells were treated with 200 μM kaempferol for 6 and 12 h (*treatment*), after which they were detached, reseeded in kaempferol-free medium and cultured for further 48 h (*recovery*). At indicated times cells were collected and counted on Thoma's chamber by optic microscopy before staining with Trypan blue. (B) Trypan blue positive cells were expressed as percentage of total cells. (C) Trypan blue negative cells were expressed as 10^4 cells/ml (bottom). Data reported represent the mean ± SD of n = 6 independent experiments.

concurring in kaempferol-induced toxicity: one occurring at early times due to decrease in glucose uptake, mainly responsible for autophagy induction; the other taking place later on, a consequence of mitochondrial OXPHOS impairment, mainly responsible for cell death.

Kaempferol-induced autophagy is mediated by AMPK/mTOR pathway. In the attempt to elucidate the molecular factor(s) responsible for the induction of autophagy, we looked at AMPK. Indeed, AMPK has been previously suggested to activate autophagy under energetic stress,[37] in order to induce catabolic processes and deactivate ATP-consuming pathways. Cells were treated with 200 μM kaempferol and phospho-activated AMPK evaluated by western blot. **Figure 8A** shows that the phosphorylated levels of AMPK increased time dependently. We then supplemented cell media with the fuel supplies previously used, and analyzed the phospho-activation of AMPK by western blot. **Figure 8B** shows that pyruvate and succinate significantly lowered the expression levels of phospho-AMPK, whereas low-glucose conditions increased phospho-active levels of AMPK already without the addition of kaempferol, confirming that AMPK activation was an event dependent on the energetic state of the cell.

To assess the role of AMPK in kaempferol-mediated effects we transfected the cells with the dominant negative form of AMPK (*AMPK-DN cells*) before treatment with 200 μM kaempferol, and analyzed the apoptotic extent cytofluorometrically. **Figure 8C** shows that after 12 h of treatment with kaempferol, cells underwent apoptosis with percentages of $SubG_1$ population close to 40%. Moreover, cytofluorimetric analyses of HeLa cells upon staining with acridine orange indicated that AMPK inhibition completely abrogated autophagy (**Fig. 8D**). Western blot of LC3 pointed out that AMPK-DN cells showed no significant increase of LC3 II immunoreactivity with respect to untreated cells, confirming that AMPK positively regulated autophagy upon treatment with kaempferol (**Fig. 8E**). Evaluation of the phosphorylation state of AMPK in AGS cells also indicated that it was activated very early upon kaempferol exposure and that its inhibition resulted in a dramatic increase of apoptotic cells (**Suppl. Fig. 2F and G**), thus strengthening the idea of a general mechanism of action for kaempferol in affecting carcinoma cell viability.

Under energetic stress, AMPK can activate autophagy by phosphorylating the mTOR-associated protein raptor, or the mTOR-upstream complex tuberous sclerosis complex 2 (TSC2).[14,38] To define a possible link between AMPK and mTOR under our experimental conditions, we evaluated the expression levels of phospho-active mTOR. **Figure 8F** shows that phospho-mTOR

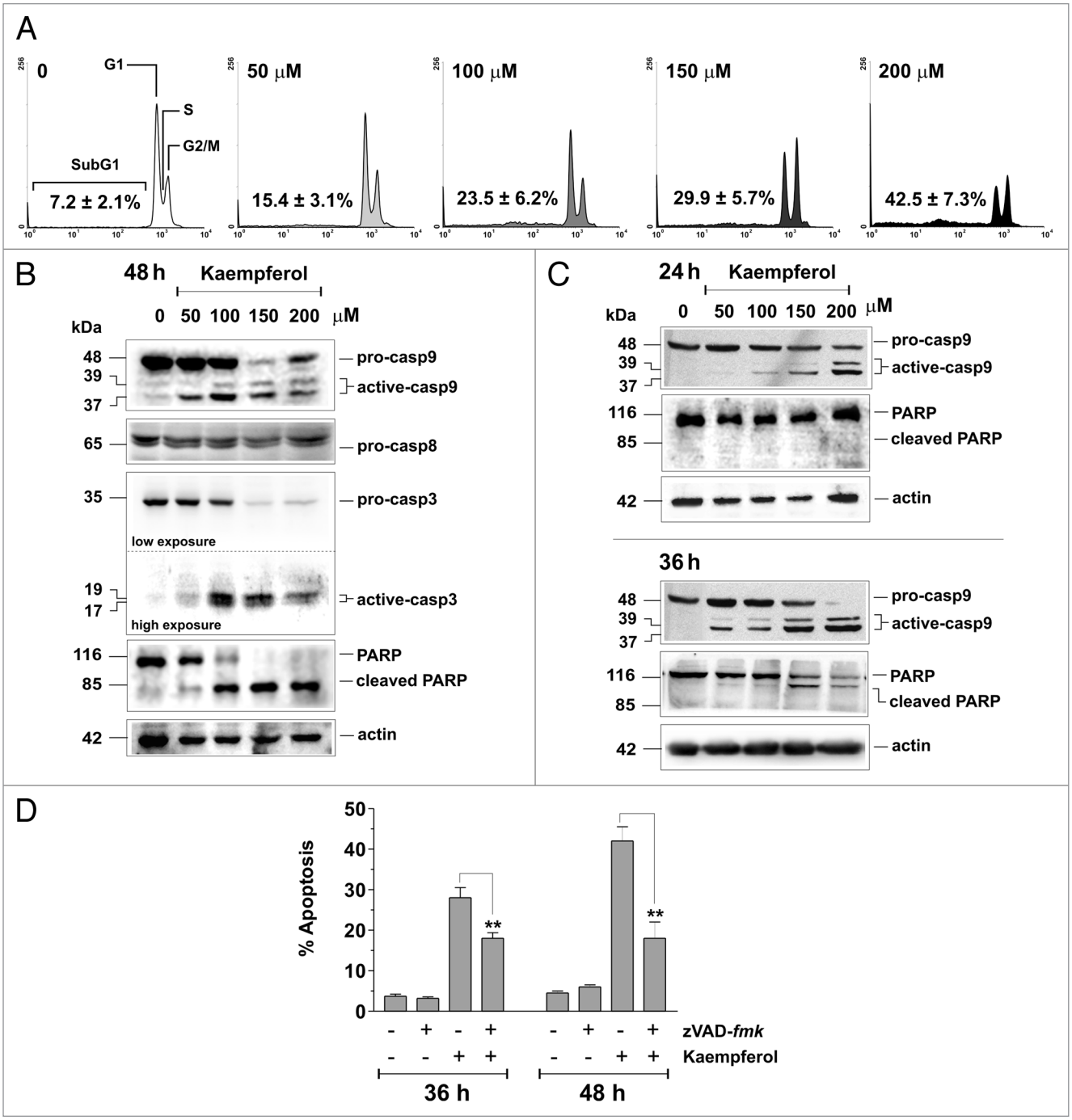

Figure 5. Effects of prolonged incubation with kaempferol on the induction of apoptosis. (A) HeLa cells were treated with 200 μM kaempferol for 48 h, washed and stained with propidium iodide. Data are expressed as percentage of apoptotic cells and represent the mean ± SD of n = 6 independent experiments. (B) HeLa cells were treated with kaempferol for 48 h. Fifty μg of total protein extract was loaded onto each lane for detection of caspase-9, caspase-8, caspase-3 and PARP. Actin was used as loading control. Due to the different specificity of the anti-caspase-3 antibody used towards cleaved and full-length form of caspase-3, two different exposures (1 min, *low* and 10 min, *high*) are shown. Western blots are from one experiment representative of three that gave similar results. (C) HeLa cells were treated with kaempferol for 24 and 36 h. Fifty μg of total protein extract was loaded onto each lane for detection of caspase-9 and PARP. Actin was used as loading control. Western blots are from one experiment representative of three that gave similar results. (D) HeLa cells were incubated for 1 h with or without 20 μM pan-caspase inhibitor zVAD-*fmk*, treated with 200 μM kaempferol for 36 and 48 h, washed and stained with propidium iodide. Data are expressed as percentage of apoptotic cells and represent the mean ± SD of n = 4 independent experiments. **p < 0.01.

decreased time dependently upon treatment with 200 µM kaempferol. In particular, HeLa cells grown in low-glucose medium showed a marked decrease of phospho-mTOR immune-reactive band already after 6 h. In support to the idea that a crosstalk between AMPK and mTOR occurred in our conditions, western blot of AMPK-DN cells indicated that phospho-mTOR was not affected by kaempferol (**Fig. 8E**).

Discussion

In this work we have dissected the antiproliferative effects of kaempferol, a member of the flavonoid subclass, in carcinoma cells. The results summarized in **Figure 9** point out a multifaceted action of this compound that impinges mainly on cellular energetics. The data demonstrate that kaempferol impedes glucose uptake and that an inverse correlation between glucose availability and cell sensitivity to kaempferol occurs. Our results are in agreement with recently published data, in which the inhibition of glucose uptake is proposed to occur upon treatment with various polyphenols.[25,26] It has been demonstrated that kaempferitrin, a diramnoside-derivative of kaempferol, directly binds to glucose transporter 4 and hinders glucose influx upon insulin stimulation.[2] However, the persistence of cell death upon pyruvate addition indicates that other pathways involved in energy production are compromised. Indeed, we found that kaempferol also induces a significant decrease of mitochondrial OXPHOS rate. Measurements of oxygen consumption pointed out that NADH-dependent respiration is inhibited by kaempferol, suggesting that it affects mitochondrial electron transfer chain at the level of Complex I. This result is further confirmed by data obtained with methyl succinate, which significantly prevents kaempferol-mediated apoptosis by supplying OXPHOS with reducible substrates at Complex II. On the basis of these results, and considering the strong similarity between the chemical structures of kaempferol and rotenone, it can be speculated that kaempferol could function by affecting electron flow at the level of the iron-sulfur cluster N2, however this aspect deserves to be deeply investigated.

The most intriguing aspect of our study is that carcinoma cells respond to kaempferol-induced bio-energetic impairment with the induction of autophagy that, in our experimental conditions, stands for a survival process. Indeed, both chemical inhibition of autophagy and siRNA against Atg5 result in an increased cell death. In the sequence of events underlying kaempferol toxicity, we demonstrate that autophagy is a reversible process that precedes the activation of cell death, because kaempferol withdrawal in the first 12 h of treatment results in the restoration of the cell capability to proliferate. Only a persistent inhibition of metabolic pathways (glycolysis and OXPHOS) can warrant the final elimination of cells via the mitochondrial apoptotic pathway. Interestingly, we found that the induction of apoptosis is a ROS-mediated and JNK-dependent event. This result corroborates many other observations that polyphenols, if added at pharmacological doses, can generate oxidative stress and induce apoptosis by the phospho-activation of MAPK family members. However, the evidence that NAC or the JNK inhibitor SP600125

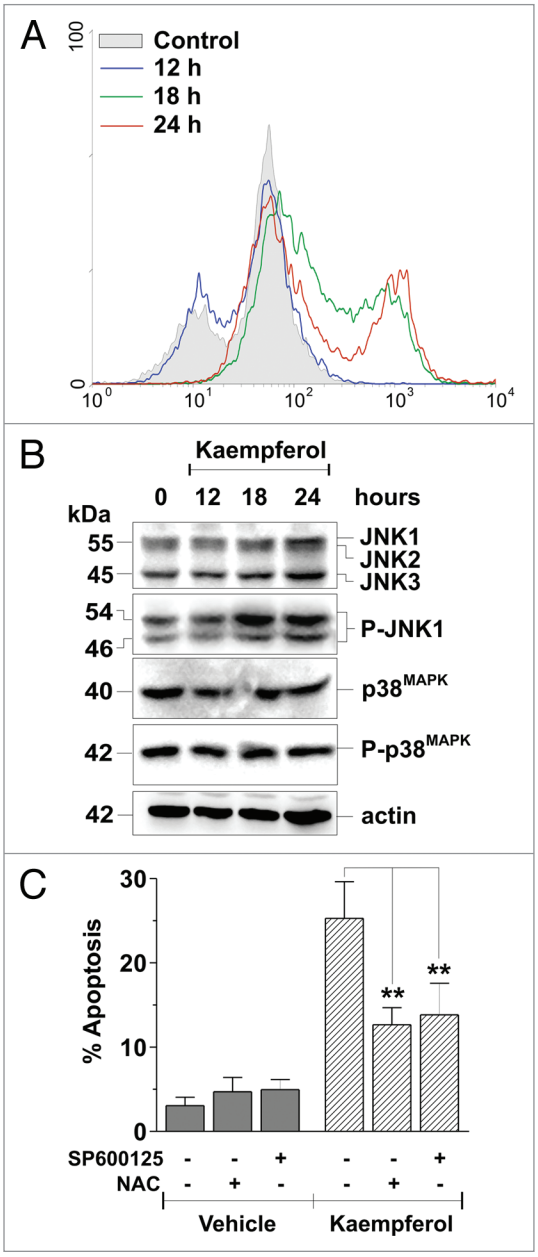

Figure 6. Role of ROS and JNK in kaempferol-induced apoptosis. (A) HeLa cells were pre-incubated for 12 h with 50 µM DCFH-DA, then treated with 200 µM kaempferol for further 12, 18 and 24 h and cytofluorimetrically analysed for intracellular ROS content. Cytofluorimetric histograms are from one experiment out of five that gave similar results. (B) HeLa cells were treated with kaempferol for 12, 18 and 24 h. Fifty µg of total protein extract was loaded onto each lane for detection of basal and phosphorylated JNK and $p38^{MAPK}$. Actin was used as loading control. Immunoblots are from one experiment representative of three that gave similar results. (C) HeLa cells were treated with 200 µM kaempferol. After 12 h, 5 mM NAC or 10 µM of the JNK inhibitor SP600125 were added and left to culture media up to 24 h, time at which cells were washed and stained with propidium iodide. Data are expressed as % of apoptotic cells and represent the mean ± SD of n = 6 independent experiments. **p < 0.01.

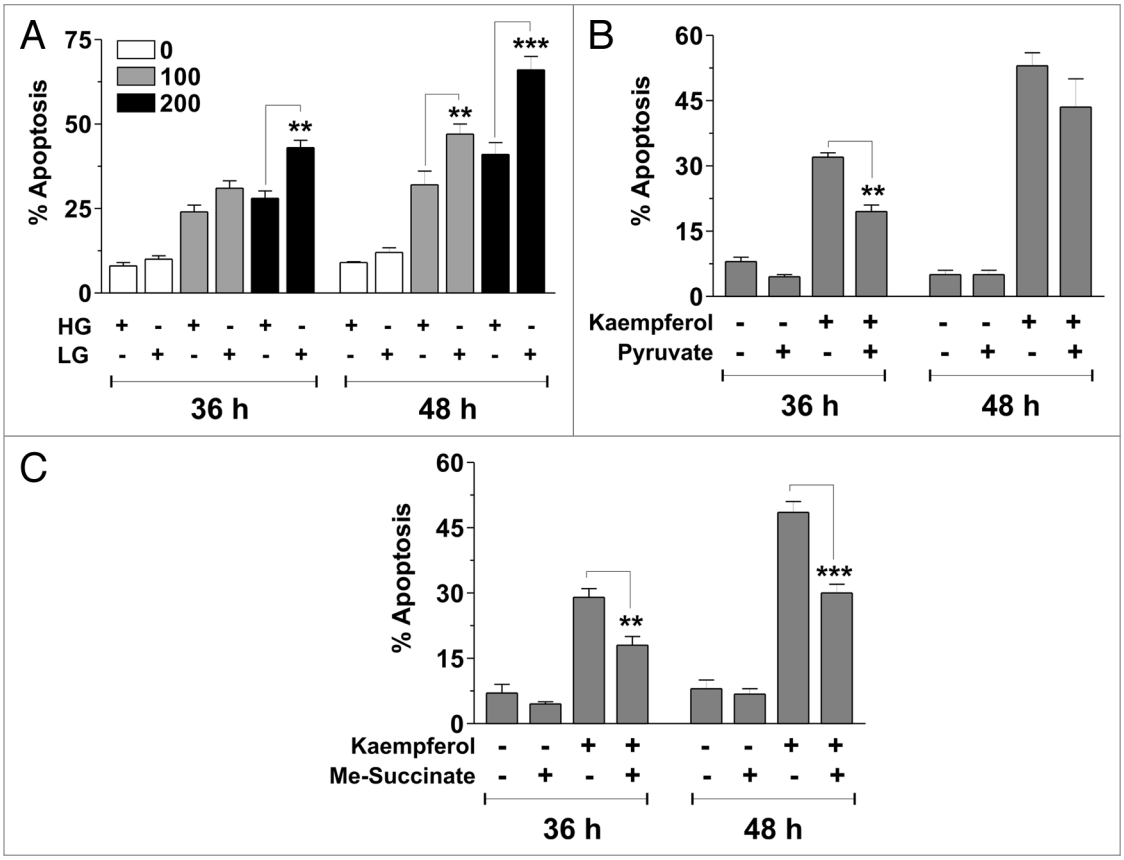

Figure 7. Effects of energetic modulation on kaempferol-induced apoptosis. (A) HeLa cells, cultured in HG or LG media were treated with 100 or 200 μM kaempferol for 36 and 48 h. Cells were washed and stained with propidium iodide. Data are expressed as percentage of apoptotic cells and represent the mean ± SD of n = 6 independent experiments. **p < 0.01; ***p < 0.001. HeLa cells were incubated for 1 h with 10 mM sodium pyruvate (B) or with 5 mM methyl succinate (*Me-succinate*) (C), treated with 200 μM kaempferol for 36 and 48 h, washed and stained with propidium iodide. Data are expressed as percentage of apoptotic cells and represent the mean ± SD of n = 4 independent experiments. **p < 0.01; ***p < 0.001.

were able to revert apoptosis even when administered 12 h after kaempferol, points out that the induction of the apoptotic program is entirely subsequent to the activation of autophagy and, reasonably, occurs when autophagy is no longer able to counter kaempferol-mediated metabolic stress. In particular, the occurrence of the only caspase-9 cleavage at 24 h of treatment with the highest dose (200 μM) of kaempferol, indicates that this time point is slightly later the borderline in which autophagy (*resistance*) switches into apoptosis (*surrender*). This is in line with recent data from literature suggesting that autophagy is commonly triggered by tumor cells to survive starvation which is occurring during uncontrolled proliferation.[39]

Among the proteins involved in survival response, we found that AMPK plays a pivotal role, being deeply involved in the induction of autophagy. It regulates catabolic and anabolic processes by sensing AMP concentration.[40] In order to maintain cellular energetic homeostasis, AMPK has been demonstrated to activate glucose uptake by enhancing transcription of the Rab GTPase Akt substrate of 160 kDa (AS160) and increase plasma membrane translocation of glucose transporter 4, as well as to increase glycolytic rate by inducing phospho-fructokinase 2 transcription. In response to metabolic stresses, it also has been suggested that AMPK activates autophagy by inhibiting mTOR pathway.[14] The results obtained in this work demonstrate that glucose consumption is affected and that the mTOR pathway inhibited upon treatment with kaempferol, thus confirming that our experimental conditions mirror those occurring upon energetic stress. In addition, artificial reduction of extracellular glucose robustly sensitizes HeLa cells to kaempferol, indicating that AMPK-elicited autophagy is mainly responsive to glucose deficiency. Conversely, the switch into apoptosis probably takes place when the mitochondrial function is compromised and the AMPK-mediated buffering response to glucose uptake inhibition is no longer sufficient to guarantee cell survival. This hypothesis is also strengthened to a great extent by apoptosis obtained upon the overexpression of the dominant negative form of AMPK, as well as by the results obtained upon incubation with pyruvate or succinate, which reinforces the assumption that a two-step process affecting cellular energetics occurs upon treatment with kaempferol.

Although our results show that kaempferol is an energetic stressor useful to inhibit proliferation of cancer cells, from a more general viewpoint, these data also provide important restrictions to the common opinion recently suggesting a promising use of polyphenols as anti-tumor compounds in virtue of their pro-oxidant properties.[23,41] Indeed, since some members of polyphenols mimic kaempferol effects, they could be able to activate autophagy

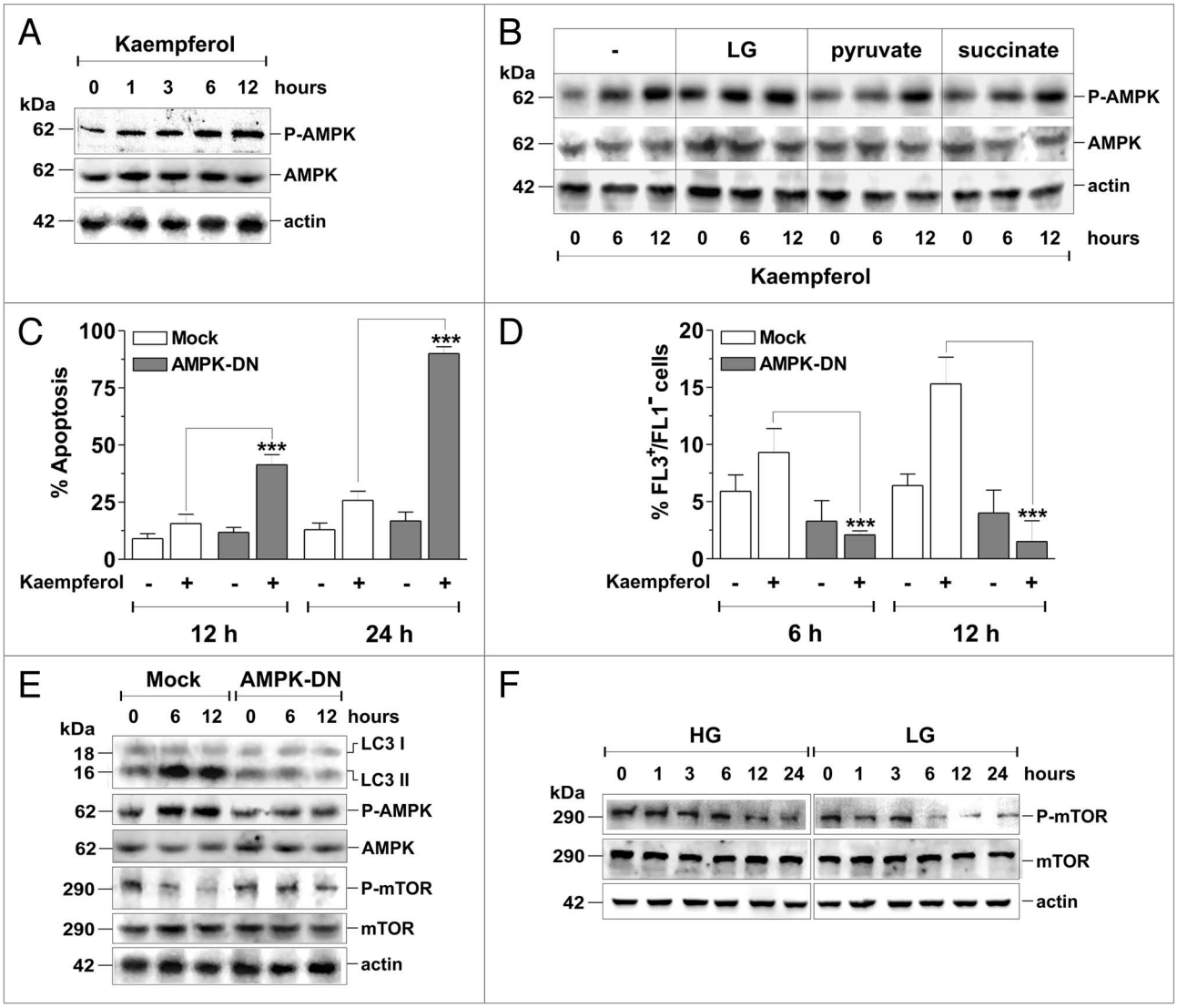

Figure 8. Pro-autophagic role of AMPK and its dependence on cellular energetic state. (A) HeLa cells were treated with 200 μM kaempferol. At indicated times, 30 μg of total protein extract was loaded onto each lane for detection of the basal and phosphorylated form of AMPK (*P-AMPK*). Actin was used as loading control. Immunoblots are from one experiment representative of three that gave similar results. (B) HeLa cells were incubated with 10 mM pyruvate or 5 mM methyl-succinate for 1 h, or grown in LG medium and then treated with 200 μM kaempferol. After 6 and 12 h, 30 μg of total protein extract was loaded onto each lane for detection of the basal and phosphorylated form of AMPK (*P-AMPK*). Actin was used as loading control. Immunoblots are from one experiment representative of three that gave similar results. (C) HeLa cells were transiently transfected with pcDNA3 empty vector (*Mock*) or with a pcDNA3 vector containing the myc-tagged coding sequence of the α2 subunit of AMPK carrying the dominant/negative mutation T172A (*AMPK-DN*). After 48 h from transfection, cells were treated with 200 μM kaempferol for 12 and 24 h. Cells were washed and stained with propidium iodide for the evaluation of apoptosis. Data are expressed as percentage of apoptotic cells and represent the mean ± SD of n = 4 independent experiments. ***p < 0.001. (D) Alternatively, after 6 and 12 h-treatment with kaempferol, cells were washed and stained with 500 nM acridine orange, for the evaluation of autophagy. Data are expressed as percentage of autophagic ($FL3^+/FL1^-$) cells and represent the mean ± SD of n = 4 independent experiments. ***p < 0.001. (E) Mock and AMPK-DN cells were treated with 200 μM kaempferol. At the indicated times, 50 μg of total protein extract was loaded onto each lane for detection of LC3-I and LC3-II, as well as basal and phosphorylated forms of AMPK and mTOR. Actin was used as loading control. Immunoblots are from one experiment representative of three that gave similar results. (F) HeLa cells, cultured in HG or LG media were treated with 200 μM kaempferol. At the indicated times, cells were lysed and 30 μg of total cell extracts were loaded for the immunodetection of the basal and phosphorylated form of mTOR. Actin was used as loading control. Immunoblots are from one experiment representative of three that gave similar results.

and enhance tumor resistance against conventional treatments, rather than rendering it more vulnerable to chemotherapies. This hypothesis is also strengthened by the knowledge of the scarce bio-availability of these molecules in vivo.[42,43] Nevertheless, our data provide a rationale for combining kaempferol with inhibitors of autophagy in the treatment of cancer progression, especially for those tumor histotypes able to activate autophagy as survival response. In addition, they highlight the great therapeutic potential of kaempferol in other human diseases, such as in the treatment of obesity. Indeed, as already suggested for other classes

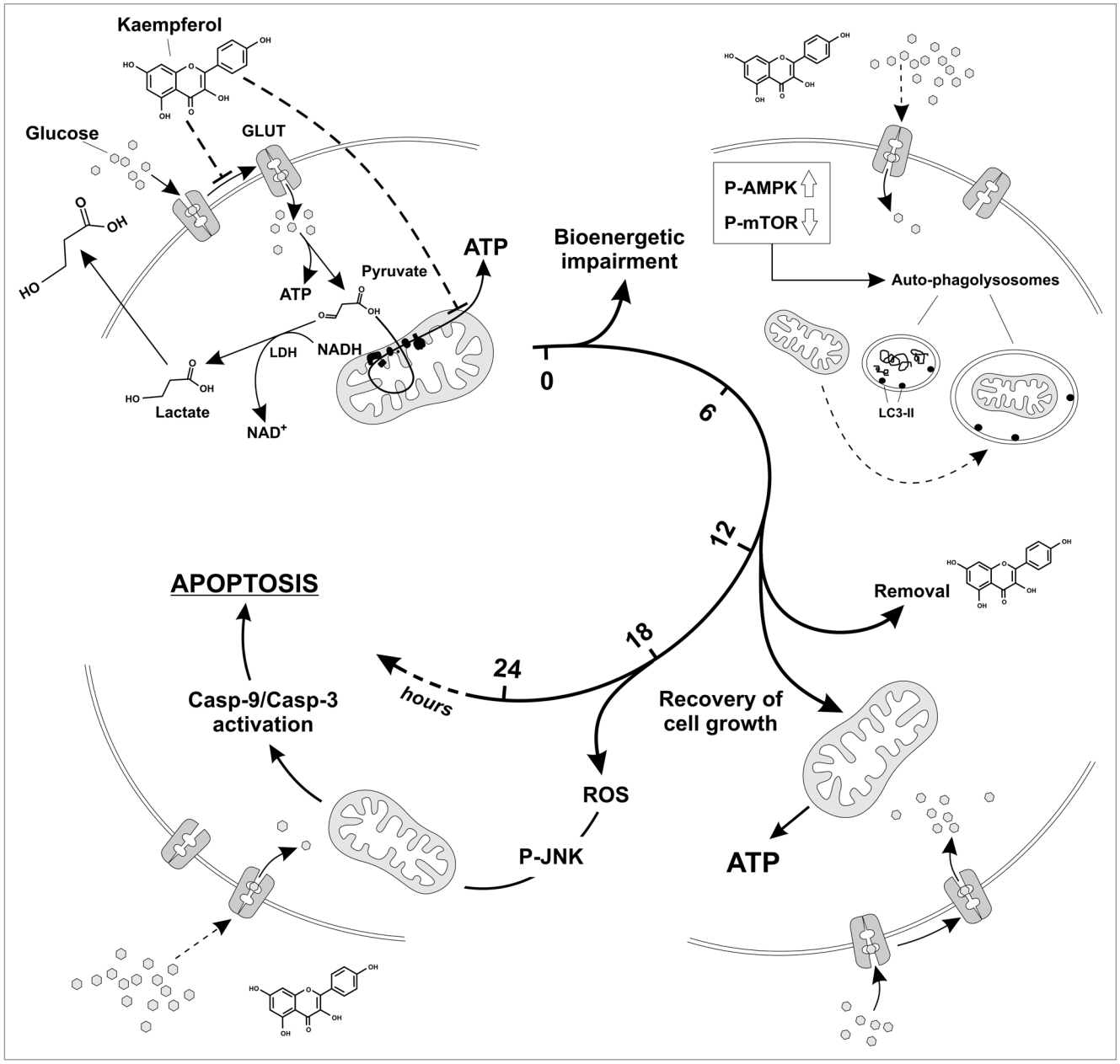

Figure 9. Model of kaempferol-induced antiproliferative effects. Kaempferol affects cellular energetics by two distinct mechanisms which occur sequentially: the earlier involves a restriction of glucose uptake and glycolysis efficiency; the latter concerns the decrease of mitochondrial respiration and ATP production. Adenocarcinoma cell lines HeLa and AGS undergo autophagy as survival response, which is reasonably maintained by increasing protein and organelle turnover, a strategy necessary for keeping tumor survival even under energetic stress. Kaempferol removal can restore normal cell growth and viability as long as it occurs within 12 h of treatment. Conversely, the exacerbation of the energetic stress results in ROS production and JNK activation, which ultimately leads the cells to activate apoptosis via the mitochondrial pathway.

of polyphenols, kaempferol might reduce glucose uptake in the intestine and function as hypo-caloric food supplement.[44,45] Kaempferol could be also useful in the treatment/prevention of neurodegenerative diseases, where self-digestion of the cells has been indicated to represent a protective process able to increase turnover of proteins and organelles.[46-48] Preliminary results from our laboratory indicate that low doses of kaempferol are still able to induce autophagy, without affecting viability of different cell lines, such as those of neuronal origin. However, additional investigations are necessary to comprehend the real efficacy of kaempferol in vivo and to assess therapeutic approaches based on the consumption of kaempferol-containing foods or the purified molecule.

Materials and Methods

Materials. Acridine orange (318337), compound C (P5499), dimethyl sulfoxide (DMSO, 154938), kaempferol (K0133),

3-methyladenine (3-MA, M9281), monensin (M5273), N-acetylcysteine (A9165), propidium iodide (P4170), methyl succinate (M81101), sodium pyruvate (S8636) and donkey anti-goat (G7767) were from Sigma. 2-[N-(7-nitrobenz-2-oxa-1,3-diazol-4-yl)amino]-2-deoxy-D-glucose (2-NBDG, N13195) and Lysotracker Red® (L7528) were from Invitrogen (San Giuliano Milanese, Italy); zVAD-*fmk* (ALX-350-020-M001) and wortmannin (ALX-260-039-M001) were from Alexis Biochemicals; JNK Inhibitor SP600125 (420119) and 2',7'-dihydrodichlorofluorescin diacetate (287810) were from Calbiochem. Goat anti-mouse (172-1011) and anti-rabbit (172-1019) and IgG (H + L)-horseradish peroxidase conjugated were from Bio-Rad (Hercules, CA); anti IgG2a (sc-2061) was from Santa Cruz Biotechnology. All other chemicals were obtained from Merck.

Cell cultures. Human epithelial and gastric carcinoma cells HeLa and AGS were purchased from the European Collection of Cell Culture, and grown at 37°C in an atmosphere of 5% CO_2. HeLa cells were cultured in DMEM containing 25 mM glucose (BE12-604F) or 5.6 mM glucose (low glucose, BE12-707F), whereas AGS were grown in F12-HAM'S (BW12-615F). All media were from Lonza and were supplemented with 10% fetal bovine serum (BE14-801F), 2 mM L-glutamine (BE17-605E), 1,000 U/ml penicillin-streptomycin (Lonza, DE17-602E).

Treatments. A 20 mM kaempferol solution was prepared by dissolving the lyophilized compounds in DMSO. Treatments were done with different amounts of kaempferol in medium supplemented with serum. As a control, equal volumes of DMSO (1%) were added to untreated cells. The pan-caspase inhibitor, zVAD-*fmk* was used at the final concentration of 20 μM. The autophagy inhibitors 3-MA, wortmannin and monensin were pre-incubated for 1 h before the addition of kaempferol and used at the final concentration of 10 mM, 1 μM and 2.5 μM, respectively. Sodium pyruvate and methyl succinate were pre-incubated for 1 h and used at the final concentrations of 10 and 20 mM, respectively. The AMPK inhibitor, Compound C was used on AGS at the final concentration of 5 μM, added 1 h before treatment with kaempferol and maintained throughout the experimental time.

Analysis of cell viability, apoptosis and autophagy. The percentages of apoptotic cells were evaluated upon staining with propidium iodide as previously described.[49] Alternatively, Trypan blue-positive cells were counted by optic microscopy. For autophagy determination, cells were incubated with 500 nM acridine orange. The increase of FL-3 emitting cells (bright red) is considered proportional to the increase of intracellular acidification, which, in turn, mostly relies upon the accumulation of autolysosomes.[31,50]

Western blot analyses. Total protein lysates were obtained as previously reported,[51] electrophoresed by SDS-PAGE and blotted onto PVDF membrane (Bio-Rad). Primary antibodies used are as follow: polyclonal anti-caspase-9 (9502), anti-phospho-Thr^{172}AMPK (2535), anti-phospho-Ser^{2448}-mTOR (2974), anti-mTOR (2983), anti-Atg5 (2630) were from Cell Signaling Technology; anti-JNK (sc-474), anti-p38^{MAPK} (sc-7149), anti-actin (sc-1615) were from Santa Cruz Biotechnology. Monoclonal anti-LC3 (0260LC3-3-2G6) was from Nanotools; anti-phospho-p38^{MAPK} (Thr180/Tyr182) (9216), anti-phospho-JNK (9255) were from Cell Signaling Technology; anti-caspase-8 (sc-70503) anti-PARP (sc-53643), anti-caspase-3 (sc-56053) anti-GAPDH (sc-47724), anti AMPK-α1/2 (sc-74461) were from Santa Cruz.

Cell transfections. Cells were transfected by electroporation using a Gene Pulser Xcell system (Bio-Rad). 24 h after plating, 50% confluent HeLa cells were electroporated with an LC3-EGFP-containing plasmid,[52] kindly provided by Prof. Francesco Cecconi, Department of Biology, University of Rome "Tor Vergata," with a pcDNA3 empty vector or with a pcDNA3 vector containing the myc-tagged coding sequence for the α2 subunit of AMPK carrying the T→A substitution at the residue 172 (kindly provided by Prof. David Carling from the Clinical Sciences Centre, Imperial College, Hammersmith Hospital, Du Cane Road, London, UK). After transfection, cells were immediately seeded into fresh medium and used after 48 h, since this time was sufficient to significantly increase the expression of this dominant/negative form of AMPK.[53] Knockdown of Atg5 expression was performed by transfecting the cells with On-TargetPlus SmartPool small interference RNA (siRNA) (Darmacon, Lafayette, CO). Controls were transfected with a scramble siRNA duplex, which does not present homology with any other human mRNAs (siScr).

Fluorescence microscopy analyses. Cells expressing EGFP-LC3 were stained with 75 nM Lysotracker Red, fixed with 4% paraformaldehyde and rapidly visualized by fluorescence microscopy. Images of cells were digitized with a Delta Vision Restoration Microscopy System (Applied Precision Inc., Issaquah, WA) equipped with an Olympus IX70 fluorescence microscope.

Oxygen consumption. Oxygen consumption of intact cells was measured by a Clark-type oxygen electrode (Gilson Medical Electronic, 3000W mod 5/6H) maintained at 37°C. Oxygen consumption by each complex was determined according to Villani and Attardi.[54] Mitochondrial oxygen consumption on intact mitochondria from mouse liver was performed as previously described.[53] Before each analysis, state IV/state III ratio was measured by adding ADP to check the integrity of mitochondrial fractions.

Extracellular lactate assay. 10 μl of trichloroacetic acid-precipitated proteins from cell media was incubated at room temperature in 290 μl of a 0.2 M glycine/hydrazine buffer, pH 9.2, containing 0.6 mg/ml NAD^+ and 17 U/ml lactate dehydrogenase. NAD^+ reduction was followed at 340 nm and nmoles of NADH formed were considered stoichiometrically equivalent to extracellular lactate.

Measurement of 2-NBDG uptake. Cells were incubated with 100 μM 2-NBDG, a fluorescent derivative of 2-deoxy-D-glucose, washed with PBS and analyzed cytofluorometrically. Alternatively, cells plated on coverslips were incubated for 30 min with 100 μM 2-NBDG and visualized by fluorescence microscopy.

ATP evaluation. ATP levels were measured by the ATP Bioluminescence Assay Kit CLS II (Roche Applied Science).

ROS evaluation. Before treatments, cells were pre-incubated with 50 μM DHDCF-DA for 12 h at 37°C. After treatments, cells were washed and resuspended in ice-cold PBS. The fluorescence intensities of DCF, formed by the reaction of DCF-DA

with ROS, were analyzed cytofluorometrically by recording FL-1 fluorescence.

Caspase 3 measurement. Cells were lysed in 100 mM Hepes, pH 7.5 0.1% CHAPS, 1 mM PMSF, 10 mM DTT and 1 mM EDTA and left on ice for 30 min. Following sonication, lysates were centrifuged at 10,000 x*g* for 10 min at 4°C. Supernatants were used for fluorometric assay of caspase-3 in lysis buffer containing the specific substrate Ac-DEVD-AFC (5 μM) at 30°C.

Protein determination. Proteins were determined by the method of Lowry et al.[55]

Data presentation. All experiments were done at least three different times unless otherwise indicated. The results are presented as means ± SD. Statistical evaluation was conducted by ANOVA, followed by Bonferroni's test. Comparisons were considered significant at $p < 0.05$.

Acknowledgements

This work was partially supported by grants from Ministero della Salute; Ministero dell'Istruzione, dell'Università e della Ricerca (MIUR); and Fondo per gli Investimenti della Ricerca di Base (FIRB) "Idee Progettuali."

Note

Supplementary materials can be found at:
www.landesbioscience.com/supplement/FilomeniAUTO6-2-Sup.pdf

References

1. Griffiths JR. Causes and consequences of hypoxia and acidity in tumour microenvironments. Bioessays 2001; 23:295-6.
2. Vishnu Prasad CN, Suma Mohan S, Banerji A, Gopalakrishnapillai A. Kaempferitrin inhibits GLUT4 translocation and glucose uptake in 3T3-L1 adipocytes. Biochem Biophys Res Commun 2009; 380:39-43.
3. Petch D, Butler M. Profile of energy metabolism in a murine hybridoma: glucose and glutamine utilization. J Cell Physiol 1994; 161:71-6.
4. Rodríguez-Enríquez S, Vital-González PA, Flores-Rodríguez FL, Marín-Hernández A, Ruiz-Azuara L, Moreno-Sánchez R. Control of cellular proliferation by modulation of oxidative phosphorylation in human and rodent fast-growing tumor cells. Toxicol Appl Pharmacol 2006; 215:208-17.
5. Coyle T, Levante S, Shetler M, Winfield J. In vitro and in vivo cytotoxicity of gossypol against central nervous system tumor cell lines. J Neurooncol 1994; 19:25-35.
6. Maher JC, Krishan A, Lampidis TJ. Greater cell cycle inhibition and cytotoxicity induced by 2-deoxy-D-glucose in tumor cells treated under hypoxic vs. aerobic conditions. Cancer Chemother Pharmacol 2004; 53:116-22.
7. Rossignol R, Gilkerson R, Aggeler R, Yamagata K, Remington SJ, Capaldi RA. Energy substrate modulates mitochondrial structure and oxidative capacity in cancer cells. Cancer Res 2004; 64:985-93.
8. Reitzer LJ, Wice BM, Kennell D. Evidence that glutamine, not sugar, is the major energy source for cultured HeLa cells. J Biol Chem 1979; 254:2669-76.
9. Bernal SD, Lampidis TJ, McIsaac RM, Chen LB. Anticarcinoma activity in vivo of rhodamine 123, a mitochondrial-specific dye. Science 1983; 222:169-72.
10. Geschwind JF, Ko YH, Torbenson MS, Magee C, Pedersen PL. Novel therapy for liver cancer: direct intraarterial injection of a potent inhibitor of ATP production. Cancer Res 2002; 62:3909-13.
11. Ko YH, Smith BL, Wang Y, Pomper MG, Rini DA, Torbenson MS, et al. Advanced cancers: eradication in all cases using 3-bromopyruvate therapy to deplete ATP. Biochem Biophys Res Commun 2004; 324:269-75.
12. Izuishi K, Kato K, Ogura T, Kinoshita T, Esumi H. Remarkable tolerance of tumor cells to nutrient deprivation: possible new biochemical target for cancer therapy. Cancer Res 2000; 60:6201-7.
13. Kato K, Ogura T, Kishimoto A, Minegishi Y, Nakajima N, Miyazaki M, et al. Critical roles of AMP-activated protein kinase in constitutive tolerance of cancer cells to nutrient deprivation and tumor formation. Oncogene 2002; 21:6082-90.
14. Steinberg GR, Kemp BE. AMPK in Health and Disease. Physiol Rev 2009; 89:1025-78.
15. Gwinn DM, Shackelford DB, Egan DF, Mihaylova MM, Mery A, Vasquez DS, et al. AMPK phosphorylation of raptor mediates a metabolic checkpoint. Mol Cell 2008; 30:214-26.
16. Havsteen BH. The biochemistry and medical significance of the flavonoids. Pharmacol Ther 2002; 96:67-202.
17. Hanasaki Y, Ogawa S, Fukui S. The correlation between active oxygen scavenging and antioxidative effects of flavonoids. Free Radic Biol Med 1994; 16:845-50.
18. Cao G, Sofic E, Prior RL. Antioxidant and prooxidant behavior of flavonoids: structure-activity relationships. Free Radic Biol Med 1997; 22:749-60.
19. Geleijnse JM, Launer LJ, Van der Kuip DA, Hofman A, Witteman JC. Inverse association of tea and flavonoid intakes with incident myocardial infarction: the Rotterdam Study. Am J Clin Nutr 2002; 75:880-6.
20. Rossi M, Garavello W, Talamini R, Negri E, Bosetti C, Dal Maso L, et al. Dietary flavonoids: bioavailability, metabolic effects and safety. Cancer Epidemiol Biomarkers Prev 2005; 16:1621-5.
21. Jiang H, Zhang L, Kuo J, Kuo K, Gautam SC, Groc L, et al. Resveratrol-induced apoptotic death in human U251 glioma cells. Mol Cancer Ther 2005; 4:555-61.
22. Sexton E, Van Themsche C, Leblanc K, Parent S, Lemoine P, Asselin E. Resveratrol interferes with AKT activity and triggers apoptosis in human uterine cancer cells. Mol Cancer 2006; 5:45.
23. Filomeni G, Graziani I, Rotilio G, Ciriolo MR. Trans-resveratrol induces apoptosis in human breast cancer cells MCF-7 by the activation of the MAP kinases pathway. Genes Nutr 2007; 2:295-305.
24. Siegelin MD, Reuss DE, Habel A, Herold-Mende C, von Deimling A. The flavonoid kaempferol sensitizes human glioma cells to TRAIL-mediated apoptosis by proteasomal degradation of survivin. Mol Cancer Ther 2008; 7:3566-74.
25. Strobel P, Allard C, Perez-Acle T, Calderon R, Aldunate R, Leighton F. Myricetin, quercetin and catechin-gallate inhibit glucose uptake in isolated rat adipocytes. Biochem J 2005; 386:471-8.
26. Nomura M, Takahashi T, Nagata N, Tsutsumi K, Kobayashi S, Akiba T, et al. Inhibitory mechanisms of flavonoids on insulin-stimulated glucose uptake in MC3T3-G2/PA6 adipose cells. Biol Pharm Bull 2008; 31:1403-9.
27. Li W, Du B, Wang T, Wang S, Zhang J. Kaempferol induces apoptosis in human HCT116 colon cancer cells via the Ataxia-Telangiectasia Mutated-p53 pathway with the involvement of p53 Upregulated Modulator of Apoptosis. Chem Biol Interact 2009; 177:121-7.
28. Jeong JC, Kim MS, Kim TH, Kim YK. Kaempferol induces cell death through ERK and Akt-dependent downregulation of XIAP and survivin in human glioma cells. Neurochem Res 2009; 34:991-1001.
29. Lagoa R, Lopez-Sanchez C, Samhan-Arias AK, Gañan CM, Garcia-Martinez V, Gutierrez-Merino C. Kaempferol protects against rat striatal degeneration induced by 3-nitropropionic acid. J Neurochem 2009; (In Press).
30. Kuma A, Matsui M, Mizushima N. LC3, an autophagosome marker, can be incorporated into protein aggregates independent of autophagy: caution in the interpretation of LC3 localization. Autophagy 2007; 4:323-8.
31. Zeng X, Kinsella TJ. Mammalian target of rapamycin and S6 kinase 1 positively regulate 6-thioguanine-induced autophagy. Cancer Res 2008; 68:2384-90.
32. Blommaart EFC, Krause U, Schellens JPM, Vreeling-Sindelárová H, Meijer AJ. The phosphatidylinositol 3-kinase inhibitors wortmannin and LY294002 inhibit autophagy in isolated rat hepatocytes. Eur J Biochem 1997; 243:240-6.
33. Petiot A, Ogier-Denis E, Blommaart EF, Meijer AJ, Codogno P. Distinct classes of phosphatidylinositol 3'-kinases are involved in signaling pathways that control macroautophagy in HT-29 cells. J Biol Chem 2000; 275:992-8.
34. Grinde B. Effect of carboxylic ionophores on lysosomal protein degradation in rathepatocytes. Exp Cell Res 1983; 149:27-35.
35. Mizushima N, Noda T, Yoshimori T, Tanaka Y, Ishii T, George MD, et al. A protein conjugation system essential for autophagy. Nature 1998; 395:395-8.
36. Fresco P, Borges F, Diniz C, Marques MP. New insights on the anticancer properties of dietary polyphenols. Med Res Rev 2006; 26:747-66.
37. Meley D, Bauvy C, Houben-Weerts JH, Dubbelhuis PF, Helmond MT, Codogno P, et al. AMP-activated protein kinase and the regulation of autophagic proteolysis. J Biol Chem 2006; 281:34870-9.
38. Lum JJ, De Berardinis RJ, Thompson CB. Autophagy in metazoans: cell survival in the land of plenty. Nat Rev Mol Cell Biol 2005; 6:439-48.
39. Mathew R, Karantza-Wadsworth V, White E. Role of autophagy in cancer. Nat Rev Cancer 2007; 7:961-7.
40. Iglesias MA, Furler SM, Cooney GJ, Kraegen EW, Ye JM. AMP-activated protein kinase activation by AICAR increases both muscle fatty acid and glucose uptake in white muscle of insulin-resistant rats in vivo. Diabetes 2004; 53:1649-54.
41. Wang IK, Lin-Shiau SY, Lin JK. Induction of apoptosis by apigenin and related flavonoids through cytochrome *c* release and activation of caspase-9 and caspase-3 in leukaemia HL-60 cells. Eur J Cancer 1999; 35:1517-25.
42. Crozier A, Jaganath IB, Clifford MN. Dietary phenolics: chemistry, bioavailability and effects on health. Nat Prod Rep 2009; 26:1001-43.
43. Wenzel E, Somoza V. Metabolism and bioavailability of trans-resveratrol. Nutrition Mol Nutr Food Res 2005; 49:472-81.

44. Cermak R, Landgraf S, Wolffram S. Quercetin glucosides inhibit glucose uptake into brush-border-membrane vesicles of porcine jejunum. Br J Nutr 2004; 91:849-55.
45. Kwon O, Eck P, Chen S, Corpe CP, Lee JH, Kruhlak M, et al. Inhibition of the intestinal glucose transporter GLUT2 by flavonoids. FASEB J 2007; 21:366-77.
46. Levine B, Kroemer G. Autophagy in the pathogenesis of disease. Cell 2008; 132:27-42.
47. Pan T, Kondo S, Le W, Jankovic J. The role of autophagy-lysosome pathway in neurodegeneration associated with Parkinson's disease. Brain 2008; 131:1969-78.
48. Winslow AR, Rubinsztein DC. Autophagy in neurodegeneration and development. Biochim Biophys Acta 2008; 1782:723-9.
49. Nicoletti I, Migliorati G, Pagliacci MC, Grignani F, Riccardi C. A rapid and simple method for measuring thymocyte apoptosis by propidium iodide staining and flow cytometry. J Immunol Methods 1991; 139:271-9.
50. Kanzawa T, Germano IM, Komata T, Ito H, Kondo Y, Kondo S. Role of autophagy in temozolomide-induced cytotoxicity for malignant glioma cells. Cell Death Differ 2004; 11:448-57.
51. Filomeni G, Cerchiaro G, Da Costa Ferreira AM, De Martino A, Pedersen JZ, Rotilio G, et al. Pro-apoptotic activities of novel isatin-Schiff base copper(II) complexes depends on oxidative stress induction and organelle-selective damage. J Biol Chem 2007; 282:12010-21.
52. Kabeya Y, Mizushima N, Ueno T, Yamamoto A, Kirisako T, Noda T, et al. LC3, a mammalian homologue of yeast Apg8p, is localized in autophagosome membranes after processing. EMBO J 2000; 19:5720-8.
53. Filomeni G, Piccirillo S, Graziani I, Cardaci S, Da Costa Ferreira AM, Rotilio G, et al. The isatin-Schiff base copper(II) complex Cu(isaepy)2 acts as delocalized lipophilic cation, yields widespread mitochondrial oxidative damage and induces AMP-activated protein kinase-dependent apoptosis. Carcinogenesis 2009; 30:1115-24.
54. Villani G, Attardi G. Polarographic assays of respiratory chain complex activity. Methods Cell Biol 2007; 80:121-33.
55. Lowry OH, Rosebrough NJ, Farr AL, Randall RJ. Protein measurement with the Folin phenol reagent. J Biol Chem 1951; 193:265-75.